



COMPARATIVE STUDY OF THREE METHODS FOR BRAIN TUMOR DETECTION AND EXTRACTION USING IMAGE SEGMENTATION TECHNIQUES

Jelena Cerovina^{1*},
Predrag Lekić¹,
Mirko Milošević²,
Petar Spalević¹,
Mile Petrović¹

¹Faculty of Technical Sciences,
University of Pristina in
Kosovska Mitrovica,
Kosovska Mitrovica, Serbia

²Academy of Technical and
Art Applied Studies,
School of Electrical and
Computer Engineering,
Belgrade, Serbia

Abstract:

Image segmentation is the process of dividing a digital image into image segments so that individual regions of interest can be analyzed and processed instead of the entire image. Image segmentation has a significant role in detecting regions of interest and extracting attributes and regions from those images. In this paper, five original grayscale abnormal MRI brain images have been processed by using image segmentation techniques for detecting and extracting regions of interest, in this case, tumors. This research described three methods of detection and extraction of tumors from abnormal MRI brain images in MATLAB: a method based on combined local threshold segmentation techniques with morphological operations for tumor detection; a method based on region splitting and merging segmentation techniques; and a method based on combined thresholding, Meyer's flooding watershed algorithm, as an image segmentation technique with morphological operations for tumor detection. Abnormal MRI brain images were preprocessed in order to obtain suitable results. Image data used in this research were obtained from Radiopedia, an educational radiology resource. The best method for detecting and extracting tumors has been determined by comparing the results of accuracy, sensitivity, F-measure, precision, MCC, dice, jaccard, and specificity. Based on the results of these measurements, it has been concluded and confirmed that the first and third methods are both equally good for detecting and extracting tumors.

Keywords:

MRI, Image Segmentation, Thresholding, Region Splitting and Merging, Watershed.

INTRODUCTION

In the medical field, magnetic resonance imaging (MRI) as one of the diagnostic methods is very often used to, for example, detect and analyze abnormal changes in brain soft tissue defined as tumors. Image segmentation and detection are very important methods used to distinguish the abnormal from the normal brain tissue and to localize, in this case, the brain tumor. Segmentation algorithms are focused on an area instead of an individual pixel. [1] Segmentation algorithms are based on similarity, which is one of the basic properties of intensity values. [2] This paper gives a comparative study of three proposed methods using image segmentation techniques for the detection and extraction of tumors from abnormal MRI brain images in MATLAB.

Correspondence:

Jelena Cerovina

e-mail:

jelena.cerovina@pr.ac.rs



Input abnormal original MRI brain images are preprocessed and improved in terms of noise reduction, smoothing, sharpening, and contrast enhancement to get some useful information about the size, shape, and location of abnormal tissue in the brain and to improve the accuracy of applied segmentation techniques. In all three methods, 2-D median filtering is used as an in-built function for reducing noise and smoothing, and local Laplacian filtering is used as an in-built function for image sharpening. The first method is based on combining local threshold segmentation techniques with morphological operations for tumor detection. The second method is based on region splitting and merging segmentation techniques, and the third method is proposed by Rajesh C. Patil and DR. A. S. Bhalchandra, which is based on combined thresholding and Meyer's watershed algorithm as segmentation techniques with morphological operations for tumor detection. [3] Images and data used in this paper were obtained from Radiopaedia, an educational radiology resource.

2. IMAGE PREPROCESSING

In preprocessing, the input MRI images are processed in different ways, such as filtering to remove or reduce noise, image sharpening, and registration to make all images comparable with each other. In this paper, in the methods, we applied image resizing to all five original input MRI images and edited the images in the same manner to obtain more accurate results. Various filters can be used for noise reduction, and in this paper we used the 2-D median filtering in-built function in MATLAB. Generally, the median filter is a non-linear operation that works so that the median filter passes through the image entry by entry and replaces the value of the center pixel with the median of the intensity values in the neighborhood of that pixel. [4] The median filter is effective when it is necessary to simultaneously remove noise and preserve edges. 2-D median filtering performs median filtering of the image in two dimensions. Each output pixel contains the medium-value 3-by-3 neighborhood around the corresponding pixel in the input image. [5] [3] In this paper, we also used an in-built function for fast local Laplacian filtering in order to increase the contrast of an image. In a fast local Laplacian filtering function, the parameter sigma characterizes the amplitude of edges in an image, and the parameter alpha controls the smoothing of details. The sigma and alpha parameters were determined experimentally based on human vision, and they are 0.3 and 0.4, respectively.

3. COMBINED LOCAL THRESHOLDING SEGMENTATION TECHNIQUE WITH MORPHOLOGICAL OPERATIONS

In the local thresholding technique, the threshold value T depends on the gray levels of $f(x,y)$ and some local image properties of neighboring pixels. The threshold operation with a locally varying threshold function $T(x,y)$ is given by Equation 1.

$$g(x, y) = \begin{cases} 1 & \text{if } f(x, y) \geq T(x, y) \\ 0 & \text{if } f(x, y) \leq T(x, y) \end{cases} \quad (1)$$

$$T(x, y) = f_0(x, y) + T_0 \quad (2)$$

Equation 1 - The threshold operation with a locally varying threshold function.

The image is the morphological opening of f , and the constant is the result of the function graythresh applied to. Morphological operations extract image features such as the shape of the region of interest or some other morphological features of an image and basically transform the image. [1] [6] Erosion and dilation are applied in this paper to detect the tumor.

All five original abnormal MRI brain images as input images are preprocessed by applying 2-D median filtering for noise reduction and smoothing and fast local Laplacian filtering for image sharpening. After that, images were resized, and different threshold values of parameters T_0 were applied to different input images in order to get accurate results for the detection of tumors and for converting grayscale images into binary images. For images I_1 , I_3 and I_4 it is applied $T_0=30$, for image I_2 it is applied $T_0=20$ and for image I_5 it is applied $T_0=0.2$. To segment out the tumor location from the image, it is required to create a binary tumor-masked window. By putting a tumor mask on dilated MRI brain images, the final image is obtained with a detected tumor. In the end, accuracy, sensitivity, specificity, the Sorensen-Dice, and the Jaccard metrics are calculated to estimate the success of the segmentation task. Accuracy (%) measures how well a binary segmentation method correctly identifies a condition in Equation 2, where TP , TN , FP , and FN denote true positive, true negative, false positive, and false negative, respectively.

$$accuracy = \frac{TP+TN}{FN+FP+TP+TN}$$

Equation 2 - Accuracy (%).



Sensitivity (%) is evaluated as the proportion of real positives that are correctly identified in Equation 3. Specificity (%) is computed as the proportion of real negatives that are correctly identified in Equation 4.

$$\text{sensitivity} = \frac{TP}{TN+FN}$$

Equation 3 - Sensitivity (%).

$$\text{specificity} = \frac{TN}{TN+FP}$$

Equation 4 - Specificity (%).

The Sorensen-Dice score is another way to measure segmentation accuracy and is computed as follows in Equation 5 and the Jaccard score has a relation with the Dice similarity as follows in Equation 6.

$$\text{dice} = \frac{2TP}{2TP+FP+FN}$$

Equation 5 - The Sorensen-Dice score.

$$\text{jaccard} = \frac{\text{dice}}{2-\text{dice}}$$

Equation 6 - The Jaccard score has a relation with the Dice.

The higher mentioned scores, the better the segmentation results. [7]

4. REGION SPLITTING AND MERGING SEGMENTATION TECHNIQUE

Region splitting and merging are segmentation techniques that are based on finding the regions of interest directly in such a way that region splitting subdivides the whole image as a single region into its subsidiary regions again and again until a condition of homogeneity is satisfied. The region-merging technique works in the opposite way to the region-splitting technique. [5]

All input MRI brain images are preprocessed in the way described in the first proposed method. We were able to segment the region of interest using the following Equation 7.

$$Q = \begin{cases} \text{TRUE} & \text{if } \sigma > a \text{ AND } 0 < m < b \\ \text{FLASE} & \text{otherwise} \end{cases}$$

Equation 7 - Segment the region of interest.

Where m and σ are the mean and the standard deviation of the pixels in a quad region, and a and b are constants. [8] In this paper, it is applied that constant a is less than 200 and constant b is greater than 5. The size of the quad regions is different for input MRI images.

The image size I_1 for the quad regions is 16. The image size for the quad regions is 16, and the image size of I_2 and I_5 for the quad regions is 2. The image size of I_3 and I_4 for the quad regions is 4. The result of the split and merge procedure is used as a mask and multiplied with the input image to detect tumors in the input MRI brain image. In the end, accuracy, sensitivity, specificity, the Sorensen-Dice, and the Jaccard metrics are calculated in the same way as they were described in the first proposed method.

5. COMBINED THRESHOLDING AND MEYER'S FLOODING WATERSHED SEGMENTATION TECHNIQUES WITH MORPHOLOGICAL OPERATIONS

According to Rajesh C. Patil and A. S. Bhalchandra, the method based on combining image segmentation techniques such as threshold and Meyer's flooding watershed algorithm with morphological operations for tumor detection is very efficient. The Meyer's flooding watershed algorithm works on a grayscale image. During the successive flooding of the gray value relief, watersheds with adjacent catchment basins are constructed. This flooding process is performed on the gradient image, i.e., the basins should emerge along the edges. This will lead to over-segmentation of the image, so the image must be preprocessed. [3] [9]

All input MRI brain images are preprocessed in the way described in the first proposed method. Threshold segmentation is based on a threshold value to turn a grayscale image into a binary image, and the value that is applied is 0.6. Meyer's flooding watershed algorithm [3] procedure is applied to a thresholded image. Finally, morphological operations are applied for tumor detection. In the end, accuracy, sensitivity, specificity, the Sorensen-Dice, and the Jaccard metrics are calculated in the same way as they were described in the first proposed method.

6. RESULTS AND DISCUSSION

This paper elaborates on different methodologies based on different image segmentation techniques and morphological operations for tumor detection and extraction, providing an insight as to which method should be utilized for a more reliable estimate of the segmentation results of the original image using accuracy, sensitivity, specificity, the Sorensen-Dice, and Jaccard evaluation factors.



The abnormal original MRI brain images of 512x512 pixels [10] have been used for tumor detection and extraction by various proposed methods. The first proposed method gives us the visualized results shown in Figure 1. According to human vision, the first proposed method gives a very efficient result.

There are 5 MRI brain tumour images over which the algorithm from the first proposed method is applied. The measurements of the abnormal MRI brain greyscale images on which the first proposed method is applied are described in Table 1. All of the MRI images are processed through the MATLAB code.

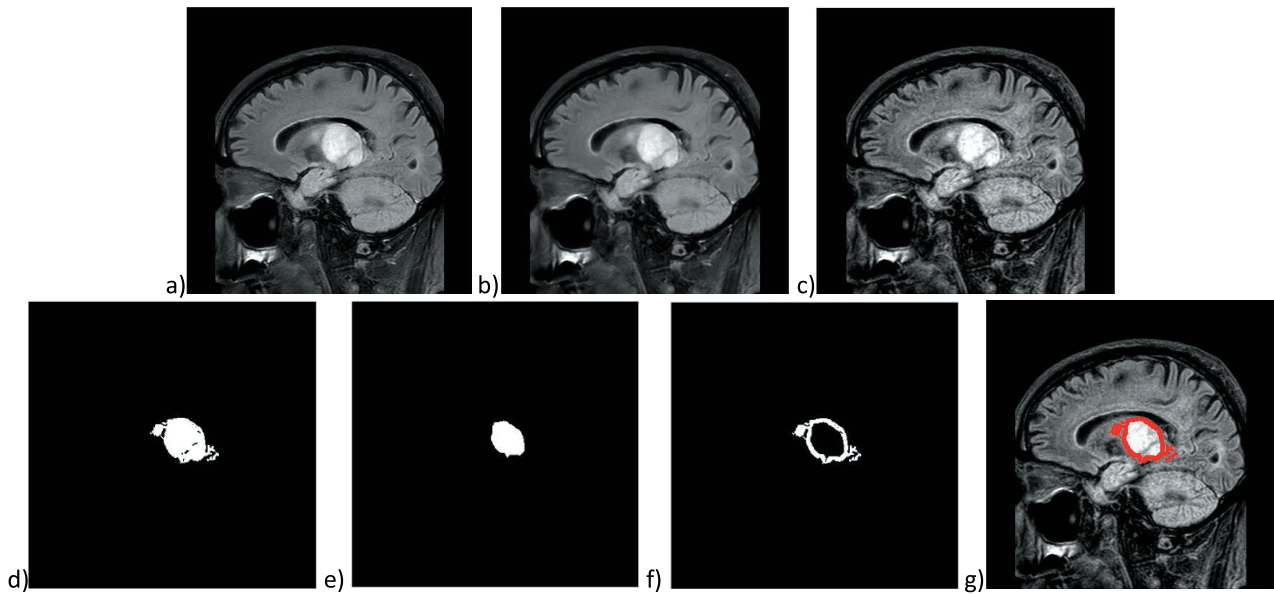


Figure 1 - a) Original abnormal MRI image, b) denoised image, c) Laplacian filtered sharpened image, d) segmented tumor, e) eroded image, f) tumor outline, g) detected tumor.

Table 1 - Resulted Accuracy, Sensitivity, Specificity, the Sorensen-Dice and the Jaccard measurements.

MRI images	Accuracy (%)	Sensitivity (%)	Specificity (%)	The Sorensen-Dice (%)	Jaccard (%)
I_1 [11]	91,99	74,27	99,97	85,20	74,22
I_2 [12]	94,91	96,99	94,50	86,17	75,70
I_3 [10]	95,92	93,97	96,82	93,55	87,88
I_4 [13]	95,29	87,90	99,73	93,38	87,58
I_5 [14]	90,53	69,41	99,86	81,79	69,19

The second proposed method gives us the visualized results shown in Figure 2. According to human vision, the second proposed method gives a less efficient result. As a final result, we obtained a segmented tumor, but there is missing information about pixels and parts of regions of normal brain tissue. The measurements of the abnormal MRI brain grayscale images on which the first proposed method was applied are described in Table 2. All of the MRI images are processed through the MATLAB code.

The third proposed method gives us the visualized results shown in Figure 5. According to human vision, the third proposed method gives a very efficient result. The measurements of the abnormal MRI brain grayscale images on which the third proposed method was applied are described in Table 3. All of the MRI images are processed through the MATLAB code.

Based on Tables 1, 2, and 3, we can conclude that the better results for accuracy, sensitivity, specificity, the Sorensen-Dice, and the Jaccard measurements are obtained by applying algorithms for the first and third proposed methods on abnormal original MRI brain images than by applying algorithms for the second method.

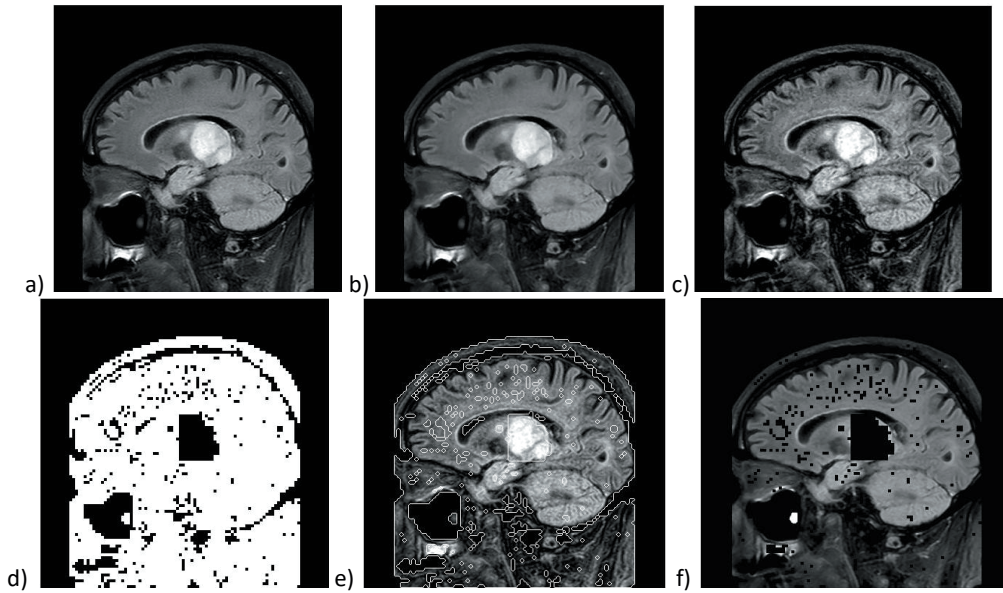


Figure 2 - a) Original abnormal MRI image, b) denoised image, c) Laplacian filtered sharpened image, d) segmented tumor by split and merge procedure, e) segmented tumor used as a mask for detection, f) detected tumor.

Table 2 - Resulted Accuracy, Sensitivity, Specificity, the Sorensen-Dice and the Jaccard measurements.

MRI images	Accuracy (%)	Sensitivity (%)	Specificity (%)	The Sorensen-Dice (%)	Jaccard (%)
$I_1[11]$	88,10	95,83	84,62	83,35	71,45
$I_2[12]$	79,46	71,44	81,02	52,22	36,26
$I_3[10]$	70,69	88,82	62,35	65,62	48,83
$I_4[13]$	81,92	98,19	71,90	80,31	67,10
$I_5[14]$	81,51	65,95	88,38	68,60	52,21

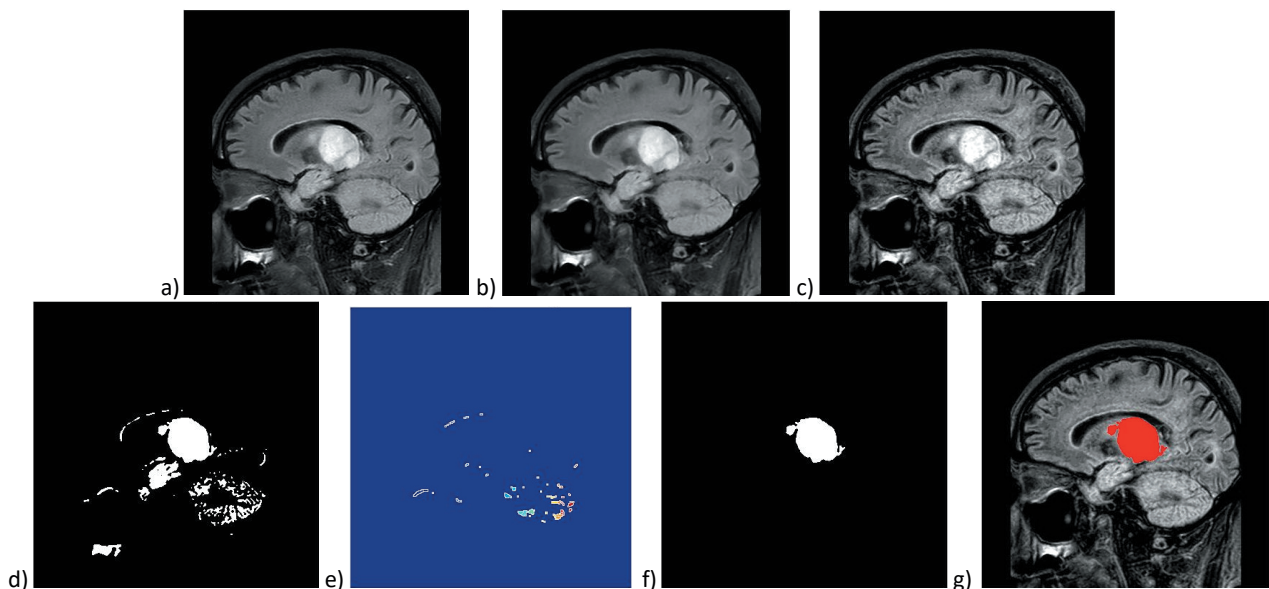


Figure 3 - a) Original abnormal MRI image, b) denoised image, c) Laplacian filtered sharpened image, d) thresholded of the whole image, e) watershed segmented image, f) only tumor segmented, g) detected tumor.



Table 3 - Resulted Accuracy, Sensitivity, Specificity, the Sorensen-Dice and the Jaccard measurements.

MRI images	Accuracy (%)	Sensitivity (%)	Specificity (%)	The Sorensen-Dice (%)	Jaccard (%)
I_1 [11]	92,16	74,84	99,97	85,58	74,79
I_2 [12]	94,40	96,52	93,99	84,95	73,84
I_3 [10]	95,06	92,52	96,22	92,18	85,49
I_4 [13]	95,13	87,64	99,78	93,13	87,14
I_5 [14]	90,88	70,73	99,78	82,61	70,38

7. CONCLUSION

Effective results for tumor detection and extraction are obtained by using algorithms following the first and third proposed methods. According to human vision, the quality, precision, and accuracy of the detected and extracted tumor applying algorithms from the first and third proposed methods are found to be better than the results given by the algorithm from the second proposed method. During the segmentation process, the internal structure of the image is preserved by applying the first and third proposed methods, and the location and area of the region of interest are accurately detected and extracted. The application of the second proposed method results in a detected and extracted region of interest whose edges are not preserved, as well as a lack of information about individual elements of the image and even parts of the surface in the internal structure of the image. Based on results obtained for accuracy, sensitivity, specificity, the Sorensen-Dice, and the Jaccard measurements, we can conclude that better results for tumor detection and extraction provide us with the first and third proposed methods.

8. REFERENCES

- [1] G. Evelin Sujji, Y.V.S. Lakshmi, G. Wiselin Jiji, "MRI Brain Image Segmentation Based on Thresholding", *International Journal of Advanced Computer Research*, Vol.3, No.1, 2013.
- [2] R. C. Gonzalez, R. E. Woods, *Digital Image Processing*, 3rd Edition, 2008.
- [3] R. C. Patil, A. S. Bhalchandra, "Brain Tumor Extraction from MRI Images using MATLAB", *International Journal of Electronics, Communication & Soft Computing Science and Engineering*, Vol. 2, Issue 1.
- [4] V. Y. Borole, S.I S. Nimbhore, S. S. Kawthekar, "Image Processing Techniques for Brain Tumor Detection: A Review", *International Journal of Emerging Trends & Technology in Computer Science*, Vol. 4, Issue 5(2), 2015.
- [5] N. Baraija, H. Modi, "Comparative Study of Different Methods for Brain Tumor Extraction from MRI Images using Image Processing", *Indian Journal of Science and Technology*, Vol. 9, DOI: 10.17485/ijst/2016/v9i4/85624.
- [6] S. Z. Oo, A. S. Khaing, "Brain Tumor Detection and Segmentation using Watershed Segmentation and Morphological Operations", *International Journal of Research in Engineering and Technology*.
- [7] D. N. H. Thanh, V. B. S. Prasath, L. M. Hien, N. N. Hien, "Melanoma Skin Cancer Detection Method Based on Adaptive Principal Curvature, Colour Normalisation and Feature Extraction with the ABCD Rule", *Journal of Digital Imaging*, vol. 33, no. 3, pp. 574–85, doi:10.1007/s10278-019-00316-x.
- [8] R. C. Gonzalez, R. E. Woods, "Digital Image Processing", 2nd Edition, 2002.
- [9] H. Zhu, B. Zhang, A. Song, W. Zhang, "An Improved Method to Reduce Over-Segmentation of Watershed Transformation and its Application in the Contour Extraction of Brain Image", *IEEE International Conference on Dependable, Autonomic and Secure Computing*, 2009.
- [10] R. Thibodeau, "Radiopaedia.org Base Image", Case ID: 164500. [Online]. Available: <https://radiopaedia.org/cases/164500?lang=gb>. [Accessed: Apr.4, 2023]
- [11] D. Ibrahim, "Radiopaedia.org Base Image", Case ID: 151153. [Online]. Available: <https://radiopaedia.org/cases/151153?lang=gb>. [Accessed: Apr.4, 2023]
- [12] R. Thibodeau, "Radiopaedia.org Base Image", Case ID: 166392. [Online]. Available: <https://radiopaedia.org/cases/166392?lang=gb>. [Accessed: Apr.4, 2023]
- [13] R. Thibodeau, "Radiopaedia.org Base Image", Case ID: 163355. [Online]. Available: <https://radiopaedia.org/cases/163355?lang=gb>. [Accessed: Apr.4, 2023]
- [14] A. I. Ranchod, "Radiopaedia.org Base Image", Case ID: 164500. [Online]. Available: <https://radiopaedia.org/cases/93234?lang=gb>. [Accessed: Apr.4, 2023]